

## **STRENGTH AND ENERGY ABSORPTION OF HIGH-STRENGTH STEEL FIBER-CONCRETE CONFINED BY CIRCULAR HOOPS**

Antonius<sup>1\*</sup>

<sup>1</sup>*Department of Civil Engineering, Sultan Agung Islamic University, Semarang 50112, Indonesia*

(Received: February 2015 / Revised: March 2015 / Accepted: April 2015)

### **ABSTRACT**

This paper presents the results of an experimental study of the behavior of high-strength steel fiber-concrete confined by hoops with round cross-sections subjected to concentric loadings. Behavior strength and energy absorption capability of confined fibrous concrete was the main focus of this study. Fibrous concrete test specimens were made by varying concrete's compressive strength and characteristics of hoops reinforcement (i.e., volumetric ratio and spacing). All specimens used longitudinal reinforcement with the same ratio. Experimental results showed that the strength enhancement of confined concrete reinforced with steel fiber is strongly influenced by the characteristics of the installed confining reinforcement. In this paper, the confinement models by researchers were evaluated and compared with the experimental results. The comparison between existing confinement models and experimental results were significantly different, especially in the post-peak behavior. Obtaining accurate characteristic predictions of high-grade confined fibrous concrete is necessary prior to modification of existing confinement models.

*Keywords:* Confinement model; Ductility; Hoops; Steel fiber; Strength

### **1. INTRODUCTION**

Concrete technology has advanced considerably, and it is now possible to produce concrete with a compressive strength of 50 MPa (i.e., high-strength concrete). High-strength concrete is more brittle than normal-strength concrete. Consequently, it requires confining reinforcement with a higher volumetric ratio, especially for the columns located in earthquake zones. Research results by Razvi & Saatcioglu (1999) and Antonius & Imran (2012) noted that when the strength of concrete in the structure of a column is higher, the strength enhancement of confined concrete (K) and ductility tend to decrease.

Various studies have been conducted to reduce the brittle nature of high-strength concrete. For example, Hadi (2009), Khalil et al. (2012), and Jansson et al. (2012) studied the confinement of concrete columns. They found that the addition of fiber in concrete mixtures would increase ductility significantly.

Steel fibers are good prospects for application because of availability and ease of manufacturing. Numerous studies have been undertaken to determine the resistance of steel fiber to high temperatures. For example, Kodur et al. (2003) and Zaidi et al. (2012) stated that the addition of steel fibers in high-strength concrete columns could improve ductility and fire endurance.

---

\* Corresponding author's email: antoni67a@yahoo.com, Tel. +62-24-6583584, Fax. +62-24-6582455  
Permalink/DOI: <http://dx.doi.org/10.14716/ijtech.v6i2.860>

Antonius et al. (2014) evaluated the resistance of concrete with steel fiber at normal and high temperatures. Results of the study showed that degradation of the compressive strength of steel fiber-concrete at temperatures over 600°C decreased extensively, even though the concrete was more ductile because of the fiber. Corrosion of steel fiber in concrete is also known to be less reactive than corrosion of the reinforcing steel. (Granju & Balouch, 2005).

The addition of fibers in concrete can significantly improve ductility, and it provides further reinforcement benefits in structures in areas that are prone to strong earthquakes. The combination of steel fiber with high-strength concrete reduces the need for mounting confining reinforcements significantly on a column. This research was conducted with the primary objective of studying the effect of several design parameters on the strength and energy absorption of confined high-strength concrete containing steel fiber. Confinement models developed by previous researchers for concrete with and without steel fiber were also evaluated. These models were analyzed in conjunction with the results of this research to determine whether the models accurately predicted the stress-strain behavior of confined high-strength steel fiber-concrete.

## 2. PREVIOUS CONFINEMENT MODELS

Table 1 presents the confinement models of fibrous concrete that can be applied to circular concrete. Generally confinement model of fiber-concrete is very ductile because of the influence of fiber in improving deformability of the concrete.

The confinement model of high-strength concrete with steel fiber was developed by Hsu and Hsu (1994) using only one stress-strain equation of confined concrete. Parameter  $\beta$  determines the shape of the stress-strain curve. Confined peak stress ( $f'_{cc}$ ) and peak strain ( $\epsilon'_{cc}$ ) of fiber-concrete were derived from empirical test results of the confining reinforcement and fiber content.

The model proposed by Mansur et al. (1997) divides the stress-strain curve into the areas before and after the peak. As in the model proposed by Hsu and Hsu, the Mansur model includes parameter  $\beta$  and also parameters  $k_1$  and  $k_2$ , which determine the shape of the stress-strain curve. Mansur's model is also proposed for high-strength fiber-concrete. The confinement model proposed by Campione (2002) is a modification of the model by Hsu and Hsu; some of the parameters that determine the slope of the stress-strain curve were modified. The parameter of  $\beta$  is based on energy absorption implemented in the  $TI$  parameter. The Campione model is also recommended for confined high-strength concrete with steel fiber. In addition to these three models, the confinement model without fiber was reviewed. The model by Mander et al. (1988) was used as a comparison because previous studies have cited it as very ductile (Antonius et al., 2013). Mander's model was developed mainly from test results on concrete columns without fiber, characterized by a normal concrete compressive strength ( $f'_c \approx 30$  MPa). Stress-strain models are proposed according to the equation shown in Table 1. The four confinement models will then be compared according to the results of experiments undertaken in this study.

## 3. EXPERIMENTAL PROGRAM

### 3.1. Materials

Concrete compressive strength ( $f'_c$ ) was designed for three groups with compressive concrete strengths of 30, 50, and 70 MPa. A cylinder with a diameter of 150 mm and a height of 300 mm was tested for 28 days according to ASTM C 39-94. Concrete material was Portland cement mixed with coarse aggregate (i.e., maximum diameter of 19 mm) and local sand. Fly ash at 15% of the weight of cement was also used in the concrete mixture. To improve the workability of fresh concrete during casting, ViscoCrete (0.7% of the weight of cement) was added.

Table 1 Confinement models

Model	Stress-strain curves	Parameter equations	Peak stress and peak strain
Hsu & Hsu (1994)	$\eta = \frac{n\beta x}{n\beta - 1 + x^{n\beta}}$	$\eta = \frac{f_c}{f'_c}; x = \frac{\varepsilon}{\varepsilon_o}$ $\beta = \frac{1}{1 - \frac{f'_c}{\varepsilon_o E_{it}}}$	For steel fiber content 0.5%: $f'_{cc} = 197.95 \rho + f'_c \text{ (in ksi)}$ $\varepsilon'_{cc} = 0.2252 \rho + \varepsilon_o$
Mansur et al. (1997)	$f_c = f_{cc} \left[ \frac{\beta \left( \frac{\varepsilon_c}{\varepsilon_{cc}} \right)}{\beta - 1 + \left( \frac{\varepsilon_c}{\varepsilon_{cc}} \right)^\beta} \right]$ $f_c = f_{cc} \left[ \frac{k_1 \beta \left( \frac{\varepsilon_c}{\varepsilon_{cc}} \right)}{k_1 \beta - 1 + \left( \frac{\varepsilon_c}{\varepsilon_{cc}} \right)^{k_2 \beta}} \right]$	$\beta = \frac{1}{1 - \frac{f_{cc}}{\varepsilon_{cc} \cdot E_{it}}}$ $k_1 = 2,77 \left( \rho_s \frac{f_y}{f_o} \right)$ $k_2 = 2,19 \left( \rho_s \frac{f_y}{f_o} \right) + 0,17$	$\frac{f_{cc}}{f_o} = 1 + 0,60 \left( \rho_s \frac{f_y}{f_o} \right)^{1,23}$ $\frac{\varepsilon_{cc}}{\varepsilon_o} = 1 + 2,6 \left( \rho_s \frac{f_y}{f_o} \right)^{0,8}$
Campione (2002)	Ascending branch: $\frac{\sigma}{f'_c} = \frac{\beta(\varepsilon/\varepsilon_o)}{\beta - 1 + (\varepsilon/\varepsilon_o)^\beta}$ Descending branch: $\frac{\sigma}{f'_c} = \eta_d \exp \left[ -k_d \left( \frac{\varepsilon}{\varepsilon_o} - x_d \right)^d \right]$	$\beta = A + B(RI)^c$ where $A = 0.5811$ $B = 1.93, C = -0.740$ $\beta = \frac{E_c}{E_c - (f'_c / \varepsilon_o)}$	$\frac{f'_{cc}}{f'_c} = 1 + 2.1 \left( k_e \frac{f_l}{f'_c} \right)^{0.7}$ $\frac{\varepsilon_{cc}}{\varepsilon_o} = 1 + 5k_1 \left( k_e \frac{f_l}{f'_c} \right)^{0.7}$
Mander et al. (1988)	$f_c = \frac{f'_{cc} x r}{r - 1 + x^r}$	$x = \frac{\varepsilon_c}{\varepsilon_{cc}} \quad r = \frac{E_c}{E_c - E_{sec}}$ $E_c = 5000 \sqrt{f'_{co}} \text{ MPa}$ $E_{sec} = \frac{f'_{cc}}{\varepsilon_{cc}}$	$\frac{f'_{cc}}{f'_{co}} = -1.254 + 2.254 \sqrt{1 + \frac{7.94 f_l}{f'_{co}}}$ $-2 \frac{f_l}{f'_{co}}$ $\varepsilon_{cc} = \varepsilon_{co} \left[ 1 + 5 \left( \frac{f'_{cc}}{f'_{co}} - 1 \right) \right]$

Materials for hoop reinforcement were plain steel bars with diameters of 5.5 mm and 6 mm and a specified yield stress ( $f_y$ ) of 415 MPa. Longitudinal reinforcement was ensured through the use of deformed bars with an effective diameter of 5.5 mm and yield stress of 430 MPa. Steel fibers were manufactured to meet a length and diameter ( $L/d$ ) ratio between 40 and 50. The steel fiber content ( $V_f$ ) was 0.5% by volume.

### 3.2. Specimens and Instrumentation

Twelve test specimens in the form of cylinders with a diameter of 125 mm and height of 310 mm included three specimens of unconfined concrete and two specimens without steel fibers. The dimensions of the test specimen were adapted to the capacity and height of tap test equipment to be used. The steel fibers and specimen reinforcements are shown in Figure 1. At the testing time to the top and bottom part, the specimen was given a sort of 5 mm thick of head piece, therefore the test region is 300 mm. To measure the axial displacement of the specimen throughout the test, Linear Variable Differential Transducers (LVDTs) were installed (100 mm maximum stroke). The LVDTs were placed in such a way to ensure the ability to measure the axial deformation of the specimens in the test region. A strain gauge type FLA-6-11 was

mounted on the longitudinal and hoops reinforcements. Further, the LVDT cables and strain gauge were connected to the Data Logger.



Figure 1 Steel fiber and reinforcement of specimens

### 3.3. Data Acquisition and Analysis of Test Data

Loading on the specimen was performed concentrically, gradually, and monotonically. An effective compression test machine with 1800 kN capacity was used for system testing and deformation control. The analysis of stress and strain on pure confined concrete was based on calculations conducted by Paultre et al. (2010) and by Antonius (2014). The loads received by concrete were obtained from an experimental load value reduced by the load received from longitudinal reinforcement. The stress of confined concrete ( $f_{cc}$ ) is defined as the load received by the concrete divided by the core cross-sectional area of the specimen. The axial strain of confined concrete ( $\epsilon_{cc}$ ) refers to the average value of the axial deformation, based on a reading of the LVDT, which was divided by the height in the test region. Strength enhancement of confined concrete ( $K$ ) is defined as the ratio between the stress of confined concrete at peak response ( $f'_{cc}$ ) with peak stress of unconfined concrete ( $f'_{co}$ ).

### 3.4. Ductility

In this research, ductility measurement is represented by the ability of confined concrete to absorb energy, which is defined as toughness. The level of toughness is expressed in the Toughness Index ( $TI$ ); calculations are carried out based on the approach by Aoude et al. (2014), as shown in Figure 2. In this image,  $TI$  is the shaded area divided by the area of the rectangle OABC.

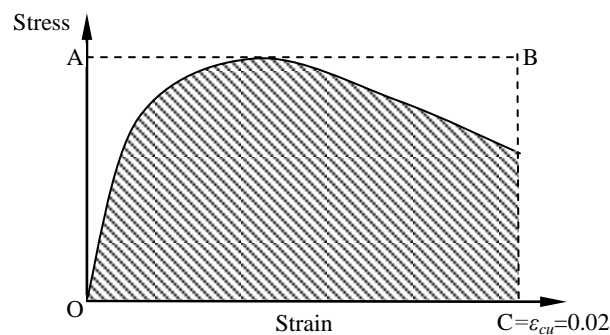


Figure 2 Toughness Index (Aoude et al., 2014)

## 4. RESULTS AND DISCUSSION

Details of the parametric designs of specimens and experimental results are shown in Table 2. UFC30, UFC50, and UFC70 specimens with steel fiber unconfined concrete were used as control specimens. Observations at the time of loading on the specimens until collapse indicated that all specimens of fibrous concrete demonstrated a relatively ductile-type collapse.

Table 2 Experimental results

Specimen	$f'_c$ (MPa)	$V_f$ (%)	Confining reinforcement		Long. Reinf.	$f'_{cc}$ (MPa)	$\varepsilon'_{cc}$	$\varepsilon_{c85}$	$K$	$TI$
			$\Phi$ - $s$ (mm)	Ratio ( $\rho_h$ )						
UFC30	29.5		-	-		-	-	-	-	-
UFC50	51.0	0.5	-	-		-	-	-	-	-
UFC70	71.2		-	-		-	-	-	-	-
FC1	51.0	0	6-60	1.58		57.00	0.0044	0.0069	1.56	0.81
FC2	71.2	0	6-60	1.58	6D5.5	79.27	0.0055	0.0094	1.31	0.78
FC3	29.5		6-60	1.58		35.25	0.0110	0.0202	1.36	0.89
FC4	29.5		6-100	0.95	$f_y =$ 430 MPa	30.22	0.0058	0.0081	1.17	0.76
FC5	51.0		6-60	1.58	415	53.50	0.0075	0.0124	1.24	0.85
FC6	51.0	0.5	6-100	0.95		48.52	0.0051	0.0095	1.12	0.61
FC7	51.0		5.5-60	1.33		55.53	0.0076	0.0120	1.28	0.74
FC8	71.2		6-60	1.58		75.58	0.0099	0.0180	1.25	0.85
FC9	71.2		5.5-60	1.33		69.49	0.0057	0.0109	1.15	0.71

For example, the FC4 specimen in Figure 3a shows that smooth cracks appeared in the surface when the loading stage reached approximately 30–40% of the peak load. The cracks grew, but not significantly, as the load increased toward its maximum. Although the post-peak response significant axial deformation occurred, failure of the specimen was well-controlled. The same behavior was observed in the FC5 specimen (Figure 3b). Results can be attributed to the role of both fiber and hoop reinforcements to slow down the collapse of the specimen and develop high ductility.

The behavior described was characteristic for all specimens. None experienced a sudden or total collapse. In general, this behavior occurs either in unconfined or confined fibrous concrete specimens.



(a) Specimen FC4



(b) Specimen FC5

Figure 3 Typical failure pattern for steel fiber-reinforced concrete

The role of fibers in improving the ductility of confined high-strength concrete is also shown in Figure 4 by comparing specimen FC1 ( $v_f = 0\%$ ,  $TI = 0.81$ ) with FC5 ( $v_f = 0.5\%$ ,  $TI = 0.85$ ), and by comparing specimen FC2 ( $v_f = 0\%$ ,  $TI = 0.78$ ) with FC8 ( $v_f = 0.5\%$ ,  $TI = 0.85$ ). As shown in the figure, the confined concrete with fiber specimens has a higher  $TI$  value.

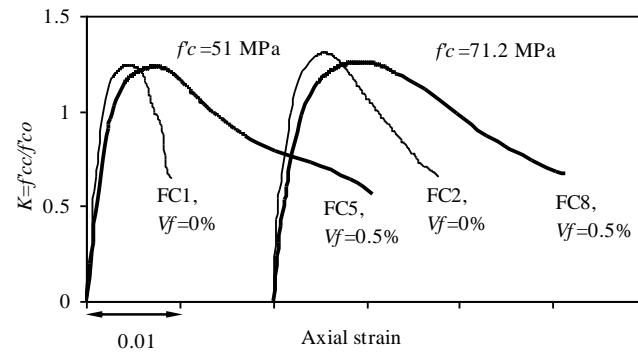


Figure 4 Influence of steel fiber on the behavior of specimens

#### 4.1. Behavior of Unconfined Concrete

In fibrous specimens, the ratios between peak stress of unconfined concrete ( $f'_{co}$ ) against the  $f'_c$  value in UFC30, UFC50, and UFC70 were 0.87, 0.85, and 0.83, respectively. Thinner specimens of unconfined concrete (with a diameter of 125 mm and height of 310 mm) compared to the standard specimen  $f'_c$  (with a diameter of 150 mm and height of 300 mm) were characterized by a  $f'_{co}$  value that was lower than  $f'_c$ . The peak strain of unconfined concrete ( $\epsilon'_{co}$ ) on each of these specimens was measured at 0.0037, 0.0035, and 0.0032. The  $\epsilon'_{co}$  value of normal-strength concrete (UFC30) was significantly higher compared to the  $\epsilon'_{co}$  value (0.002) that is usually assumed for normal concrete (without fibers). This value shows the effect of adding fiber to concrete's ability to deform significantly. The behavior of the specimen of unconfined concrete (Figure 5) also shows that consistency of ductility decreased with the increasing compressive strength of steel fiber-concrete used.

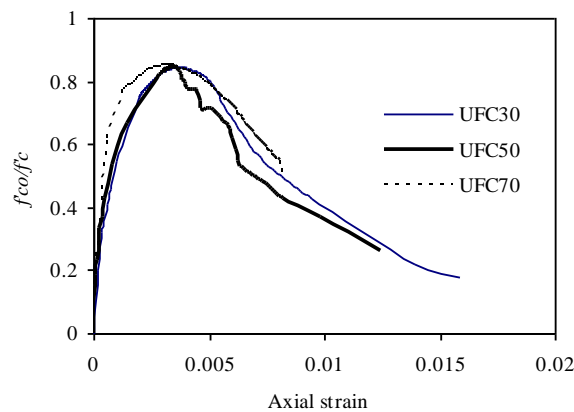


Figure 5 Stress-strain behavior of unconfined steel fiber-reinforced concrete

#### 4.2. Influence of Concrete Strength ( $f'_c$ )

The effect of different concrete compressive strengths on strength and ductility was determined by comparing specimens with characteristics similar to concrete with hoop reinforcement (space, volumetric ratio, and yield stress). Refer to Figure 6.

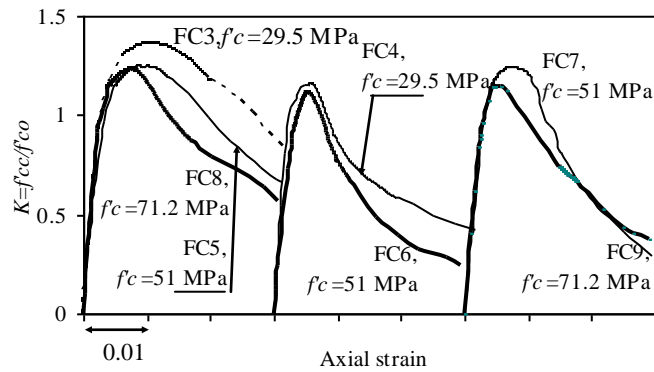


Figure 6 Influence of concrete strength on the behavior of specimens

As with normal concrete (without fibers), the effect of an increase in compressive strength of fibrous concrete was a declining trend in the value of  $K$ . In line with the increasing influence of concrete’s compressive strength, energy absorption of confined concrete also showed a decreasing trend in  $TI$  value (Table 2). The curve comparison in Figure 6 shows that if concrete strength for the specimens increases, the value of  $K$  ductility in fibrous concrete decreases. This behavior resembles that of normal concrete. These results are in line with findings of Antonius & Imran (2012).

**4.3. Influence of Spacing**

Spacing of hoops for confinement plays an important role in determining the values of  $K$  and  $TI$ . The effect of spacing on stress-strain behavior affects the fibrous concrete collapse mode. Figure 7 represents a comparison between specimens with 60 mm spacing and 100 mm spacing of reinforcing hoops. The compressive strength of concrete, the reinforcement ratio, and yield stress are the same. The narrower spacing of hoops for reinforcement is very influential in increasing the value of  $K$  and ductility of confined concrete ( $TI$  value), as shown in Table 2.

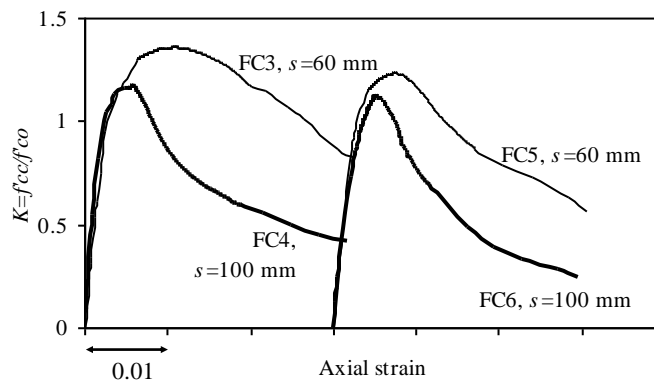


Figure 7 Influence of spacing on the behavior of specimens

**4.4. Influence of Volumetric Ratio**

Figure 8 shows the influence of the volumetric ratio of hoops on strength and energy absorption of confined fibrous concrete. As shown in that figure and Table 2, the ductility of specimens increases when the volumetric ratio of the installed hoop reinforcement increases.

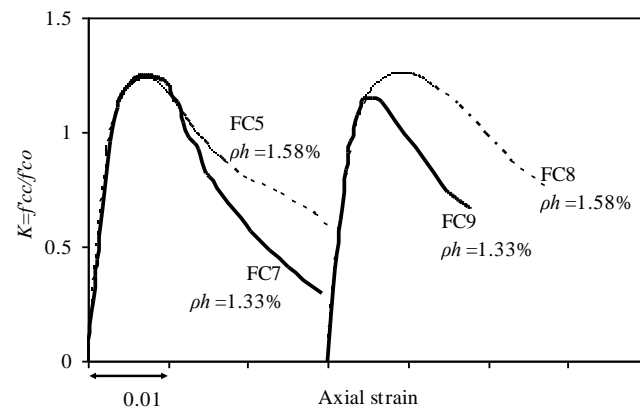


Figure 8 Influence of volumetric ratio on the behavior of specimens

## 5. COMPARISON OF CONFINEMENT MODELS WITH EXPERIMENTAL RESULTS

In this paper, confinement models in Table 1 are compared with the experimental results of this study. Figure 9 compares normal-strength concrete ( $f'_c = 29.5$  MPa) specimens, namely FC3 and FC4. The value of peak stress of confined concrete ( $f'_{cc}$ ) based on the Mansur model coincides with the values in FC3 and FC4  $f'_{cc}$  specimens. In addition, this model is able to predict the behavior of the post-peak FC3 specimen accurately, but results were significantly different for the FC4 specimen.

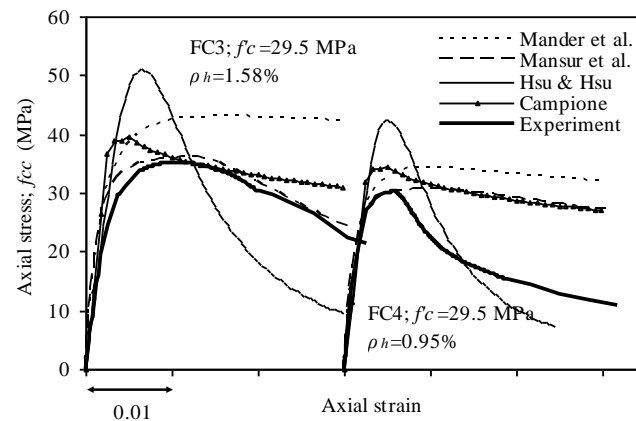


Figure 9 Comparison of confinement models with FC3 and FC4 specimens

A comparison of the stress-strain behavior of steel fiber-concrete in various confinement models was performed in another experiment using medium-strength concrete ( $f'_c = 51$  MPa), as shown in Figure 10. Accordingly, the values of  $f'_{cc}$  in FC5 and FC6 specimens of the mansur model are relatively similar to the experimental  $f'_{cc}$  values. Nevertheless, the post-peak behavior predicted for the confinement models differed significantly from the experimental results. Another comparison is shown in Figure 11 for high-strength steel fiber-concrete. According to the figure, predictions regarding  $f'_{cc}$  value and post-peak behavior of the confinement models differ significantly from experimental results.

Figures 10 and 11 show another phenomenon of post-peak behavior based on the model of Hsu and Hsu, which is non-linear and concave. It looks similar to the curve of the experimental results, although the model used by Hsu and Hsu is still too conservative (steep). However, it is

important to know that the ductility behavior of confined concrete with steel fiber for medium and high-strength concrete is non-linear and concave.

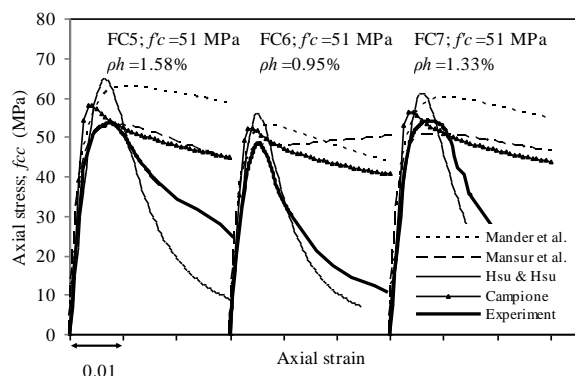


Figure 10. Comparison of confinement models with FC5, FC6, and FC7 specimens

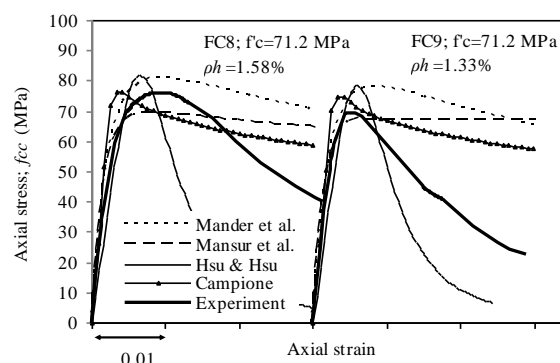


Figure 11. Comparison of confinement models with FC8 and FC9 specimens

## 6. CONCLUSION

The enhancement of the strength and ductility of confined concrete with steel fiber tends to increase when the use of concrete compressive strength is decreased, as well as when hoop reinforcement is characterized by space reduction and a higher volumetric ratio. This phenomenon is similar to that of confined normal concrete (concrete without fiber). The combination of steel fiber-concrete and the installation of hoops for reinforcement is excellent for improving the deformability of high-strength concrete. The prediction of peak stress of confined concrete with normal-strength steel fiber is based on the Mansur model with good experimental results; however, ductility is significantly different when the volumetric ratio of the reinforcing hoops is very low. In this study, the confinement models differ significantly in terms of strength and ductility from the experimental models using medium and high-strength steel fiber-concrete. Therefore, modification or development of the confined high-strength steel fiber-concrete model was necessary to predict experimental results. In this study, other types of cross-sections (i.e., squares) as well as variables of confining reinforcement, such as reinforcement configuration and yield stress, were reviewed.

## 7. ACKNOWLEDGEMENT

The experimental program presented in this paper is part of the Competitive Research Program, Contract No.002/K6/KL/SP/PEN/2014, funded by the Directorate General of Higher Education, Ministry of Education and Culture, Republic of Indonesia. The support received for this research is gratefully acknowledged.

## 8. REFERENCES

- Antonius, 2014. Performance of High-strength Concrete Columns Confined by Medium Strength of Spirals and Hoops. *Asian Journal of Civil Engineering*, Volume 15(2), pp. 245–258
- Antonius, Imran, I., 2012. Experimental Study of Confined Low-, Medium- and High-strength Concrete Subjected to Concentric Compression. *ITB Journal of Engineering Science*, Volume 44(3), pp. 252–269

- Antonius, Imran, I., Widhianto, A., 2013. Ductility of Confined Bridge Piers in the Seismic Region. *Proceeding of the 6<sup>th</sup> Civil Engineering Conference in Asia Region*, Jakarta, August 20-22, Paper ID. 039
- Antonius, Karlinasari, R., Darmayadi, D., 2014. Confinement Model for Steel Fiber Concrete. *Report of Competitive Research, Directorate General of Higher Education* (in Indonesian)
- Antonius, Widhianto, A., Darmayadi, D., Asfari, G.D., 2014. Fire Resistance of Normal and High-strength Concrete with Contains of Steel Fibre. *Asian Journal of Civil Engineering*, Volume 15(5), pp. 655–669
- Aoude, H., Hosinie, M.M., Cook, W.D., Mitchell, D., 2014. Behavior of Rectangular Columns Constructed with SCC and Steel Fibers. *Journal of Structural Engineering*, September
- ASTM C 39–94, 1996. Test Method for Compressive Strength of Cylindrical Concrete Specimens. *Annual Books of ASTM Standards*. USA
- Campione, G., 2002. The Effects of Fibers on the Confinement Models for Concrete Columns. *Canadian Journal of Civil Engineering*, Volume 29, pp. 742–750
- Granju, J-L., Balouch, S.U., 2005. Corrosion of Steel Fiber Reinforced Concrete from the Cracks. *Cement and Concrete Research*, Volume 35, pp. 572–577
- Hadi, M.N.S., 2009. Reinforcing Concrete Columns with Steel Fibers. *Asian Journal of Civil Engineering*, Volume 10(1), pp. 79–95
- Hsu, L.S., Hsu, C.T., 1994. Stress-strain Behavior of Steel-fiber High-strength Concrete under Compression. *ACI Structural Journal*, Volume 91(4), pp. 448–457
- Jansson, A., Lofgren, I., Lundgren, K., Gyltoft, K., 2012. Bond of Reinforcement in Self-compacting Steel-fiber-reinforced Concrete. *Magazine of Concrete Research*, Volume 64(7), pp. 617–630
- Khalil, W.I., Gorgis, I.N., Mahdi, Z.R., 2012. Behavior of High Performance Fiber Reinforced Concrete Columns. *ARP Journal of Engineering and Applied Sciences*, Volume 7(11), pp. 1455–1467
- Kodur, V.K.R., Cheng, F.P., Wang, T.C., Sultan, M.A., 2003. Effect of Strength and Fiber Reinforcement on Fire Resistance of High-strength Concrete Columns. *Journal of Structural Engineering*, Volume 129(2), pp. 253–259
- Mander, J.B., Priestley, M.J.N., Park, R., 1988. Theoretical Stress-strain Model for Confined Concrete. *Journal of Structural Engineering*, Volume 114(8), pp. 1804–1824
- Mansur, M.A., Chin, M.S., Wee, T.H., 1997. Stress-strain Relationship of Confined High-strength Plain and Fiber Concrete. *Journal of Materials in Civil Engineering*, Volume 9(4), pp. 171–179
- Paultre, P., Eid, R., Langlois, Y., Lévesque, Y., 2010. Behavior of Steel Fiber-reinforced High-strength Concrete Columns under Uniaxial Compression. *Journal of Structural Engineering*, Volume 136(10), pp. 1225–1235
- Razvi, S.R., Saatcioglu, M., 1999. Confinement Model for High-strength Concrete; *Journal of Structural Engineering*, Volume 125(3), pp. 281–289
- Zaidi, K.A., Sharma, U.K., Bhandari, N.M., 2012. Effect of Temperature on Uniaxial Compressive Behavior of Confined Concrete. *Fire Safety Journal*, Volume 48, pp. 58–68